Ultrathin Carbon Nanotube Fibrils of High Electrochemical Capacitance

Jun Ma,[†] Jie Tang,[†,*] Han Zhang,[†] Norio Shinya,[†] and Lu-Chang Qin[‡]

[†]1D Nanomaterials Research Group, National Institute for Materials Science, Tsukuba, Ibaraki 305-0047, Japan, and [‡]Department of Physics and Astronomy, University of North Carolina at Chapel Hill, Chapel Hill, North Carolina 27599-3255

ABSTRACT We have assembled single-wall carbon nanotubes into ultrathin long fibrils using a dielectrophoretic technique and studied the mechanical and electrochemical properties of carbon nanotube fibrils. The diameter of the fibrils can be controlled in the range of 200 nm to 2 μm, and the length can reach as long as 1 cm. The obtained fibrils have a tensile strength of about 65 MPa, electrical conductivity ranging from 80 to 200 S cm^{-1}, and specific capacitance more than 200 F g^{-1}. The results indicate that these ultrathin long carbon nanotube fibrils are of great potential for applications as conductive wires and probe electrodes.

KEYWORDS: carbon nanotube · fibril · conductivity · specific capacitance

Carbon nanotubes (CNTs), especially single-walled carbon nanotubes (SWNTs), have attracted a tremendous amount of interest in both fundamental research and technological development because of their unique nanostructures and extraordinary properties.[1−5] Extensive studies have shown that SWNTs have excellent mechanical, chemical, electrical, and electromechanical properties fitting for many applications.[6−9] For example, their unique properties have led to proposed applications in a wide range of fields including probe electrodes, biosensors, nanoelectronics, reinforced, and/or conductive polymer nanocomposites, which often require carbon nanotubes in the form of fibrils and/or films.[10−12] Recently, there has emerged a great interest in biocompatible CNT fibrils, due to their unique electronic, electrical, and mechanical properties. Most of the experimental methods for preparing CNT fibrils can be divided into two basic classes: liquid- and solid-state spinning.[12−14] In addition, other methods such as phase separation have also been reported to produce macroscopic SWNT fibrils.[15] Among the spinning techniques, liquid-spinning needs dispersing CNTs in solvents at first. In addition, wet-spinning can also produce CNT−polymer composite fibrils. For example, Wallace and his group reported that CNT fibers containing biopolymers prepared using a wet-spinning method had excellent mechanical strengths (about 100 MPa) and high electrical conductivity (100−500 S cm^{-1}).[16−18] Besides the potential applications as electrical conductors, these composite CNT fibers can also be used as actuating materials due to their electromechanical properties.[16] The fibrils produced by the wet-spinning method are usually glued together by polymers, and their diameter is typically larger than 20 μm. Fabrication of thinner CNT fibrils requires alternative techniques. Herein, we report the preparation of long SWNT fibrils with diameter smaller than 1 μm using a dielectrophoretic technique. The dielectrophoretic technique has often been used to attach short SWNT bundles on scanning probes.[19−23] This method has also been used to separate metallic from semiconducting SWNTs.[24] In this work, we report our study on morphological, mechanical, and electrical properties of such thin CNT fibrils prepared by dielectrophoresis.

RESULTS AND DISCUSSION

We have improved the dielectrophoretic method to assemble bundles of SWNTs dispersed in pure water into long carbon nanotube fibrils. In our method, an alternating current (AC) electric field drives the SWNT bundles in water toward a sharp tungsten needle tip, which had already been dipped into the suspension. When the tungsten needle tip is drawn away from the suspension at a certain speed, a meniscus is formed between the tungsten tip and the suspension. The tensile forces of the meniscus push the CNT bundles together to form a fibril on the tip. As the tungsten needle was pulled further, the SWNTs in the water are assembled continuously into a long

*Address correspondence to tang.jie@nims.go.jp.

Received for review July 12, 2009 and accepted October 26, 2009.

Published online October 30, 2009.
10.1021/nn900787h CCC: $40.75

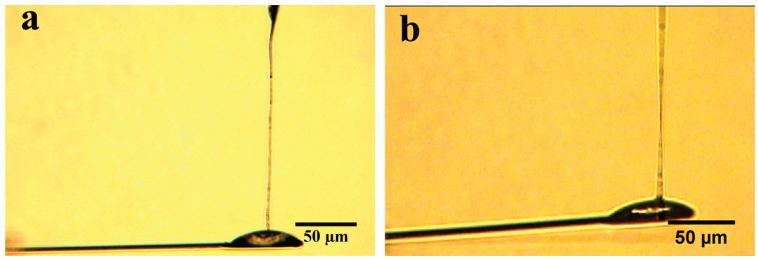

Figure 1. Optical microscopic images of a SWNT fibril during test of mechanical tension. (a) Before the test, one end of the fibril is attached onto a tungsten tip; the lower end is immersed in glue at the end of the silicon cantilever. (b) Cantilever is pulled upward by moving the tungsten tip until the fibril is broken.

fibril. After the water in the fibril is dried out in air, the bundles of SWNTs are bonded *via* van der Waals forces.[19] By varying the operation parameters, such as the concentration of SWNTs in the solution, the drawing speed, the applied voltage, and the AC frequency, a SWNT fibril can be produced to a length of several millimeters when desired. On the other hand, because these fibrils are assembled by pure SWNTs without any additive agents, they are expected to retain a significant portion of the mechanical and electrical properties of the pristine carbon nanotube material. The ideal tensile strength of SWNTs can reach 100 GPa. However, it will decrease dramatically to below 1 GPa for SWNT fibrils. The raw SWNTs (purchased commercially from Cheap Tubes, Inc.) have a conductivity of more than 100 S cm^{-1}, which is much lower than the calculated conductivity (10^4 S cm^{-1}) of the metallic SWNTs because the starting SWNTs usually contain only one-third of metallic SWNTs.[14]

The diameter of the fibrils can be easily tuned from 200 nm to 2 μm by controlling the concentration of CNTs from 0.01 to 0.1 mg mL^{-1} in the suspension. Besides the CNT concentration, the drawing speed (15−300 μm s^{-1}) is also effective in affecting the diameter of the formed fibrils, although it is not very sensitive. We should also note that, since the ultrathin fibrils (less than 200 nm in diameter) are fragile and easy to break in air, it is very challenging to recover experimentally an ultrathin fibril longer than 100 μm.

The SWNT fibrils have a typical tensile strength from 20 MPa to 1.8 GPa, and they were measured on CNT fibers of diameter larger than a few micrometers.[14,17,18] To the best of our knowledge, no experimental data have been reported for the ultrathin fibrils prepared by dielectrophoresis. In order to measure the tensile force of the SWNT fibrils that is estimated to be 0.1−10 μN, we used a special setup consisting of a rectangular cantilever beam of spring constant 0.1 N m^{-1} and a micromanipulation system. In this experiment, as shown in Figure 1a, one end of the SWNT fibril is fixed on the cantilever by epoxy resin. By pulling the cantilever slowly, as illustrated in Figure 1b, the tensile strength of the SWNT fibril is obtained when the CNT fibril is broken by the applied tensile force. At the same time, the displacement of the holding point on the cantilever was also monitored by a microscope and recorded in a movie. From the recorded frames in the movie, the bending displacement of the cantilever is then converted to the tensile force. The diameter of the tested fibril was measured from scanning electronic microscope (SEM) images, and the cross section was taken as circular and uniform along the fibril axis. Three samples have been tested successfully using this method. The tensile strength of these fibrils was estimated to be about 65 MPa by observing the displacement of a calibrated cantilever. For example, for a fibril with a diameter of about 200 nm, it displaced the cantilever by more than 20 μm before it broke.

The CNT fibrils were also examined in SEM. The SEM images of two fibrils are shown in Figure 2. One fibril has a diameter of 918 nm, and the other is 184 nm. The surface morphology of the thicker fibril is different from that of the thinner one. The SWNT bundles can be seen along the axis, as shown in Figure 2b,d. It is easier to distinguish the SWNT bundles on the thicker fibril. Thinner fibril is usually packed together by SWNT bundles more densely.

We also characterized the electrochemical properties of these conductive fibrils in a biological environment. We used an electrolyte solution of 0.2 M

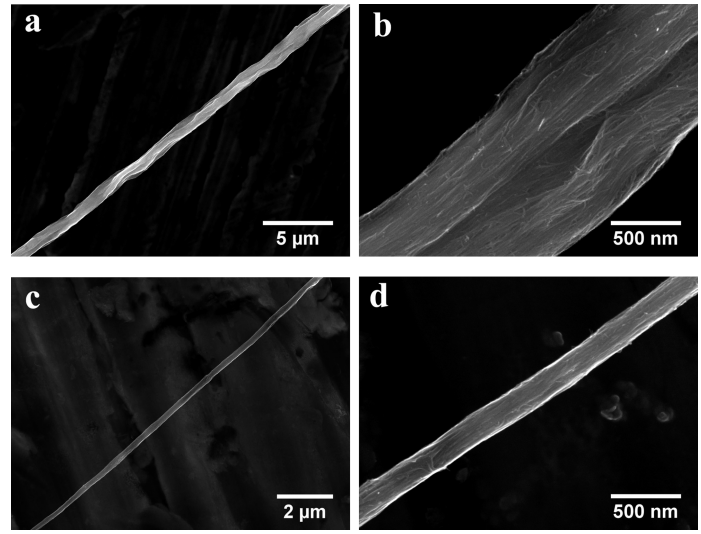

Figure 2. SEM images of SWNT fibrils drawn from SWNT−water suspension by dielectrophoresis under the following two typical conditions: (a) CNT fibril of diameter D = 918 ± 88 nm; SWNT concentration = ~0.1 mg mL^{-1}; drawing speed = 15 μm s^{-1}. (b) Magnified image of a selected portion of (a). The CNTs are aligned in the axial direction of the fibril. (c) CNT fibril of diameter D = 184 ± 10 nm; SWNT concentration = ~0.02 mg mL^{-1}; drawing speed = 30 μm s^{-1}. (d) Magnified image of a selected portion in (c). The surface appears smoother than that shown in (b).

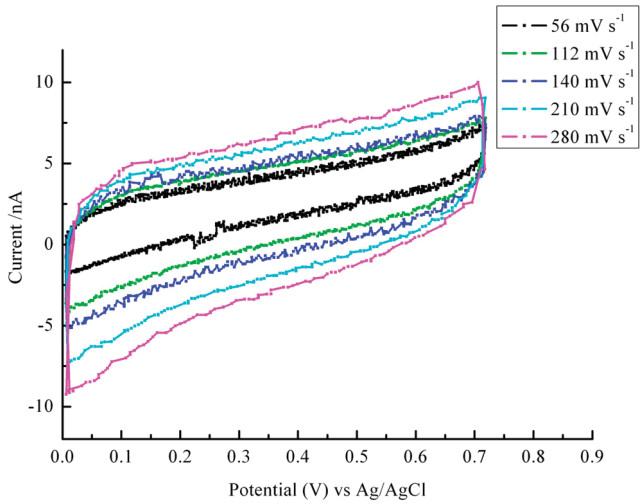

Figure 3. Cyclic voltammograms of a SWNT fibril measured in 0.2 M PBS (pH 7.4) solution at a series of scan rates (from top to bottom): 56, 112, 140, 210, and 280 mV s^{-1}.

phosphate-buffered saline solution (PBS, pH 7.4).[9,17,25] Cyclic voltammetric (CV) measurements gave a specific capacitance of above 200 F g^{-1} even at a very high scan rate (Figure 3). When the scan rate is 140−168 mV s^{-1}, the specific capacitance is about 210 F g^{-1} for this sample. The obtained CVs are featureless voltammograms, and no Faradic peaks were observed between 0 and 0.6 V. Only rectangular cyclic voltammograms over a wide range of scan rates were observed. The current plateau (at 0.4 V) increased as the scan rate increased. The CV results indicate that the charging and discharging processes are very fast at the interface between the fibril and the electrolyte solution. In addition, the CNT fibrils are stable on cycling, and no significant difference was ever observed after continuous cycles during the experiment of more than 2 h.

The high specific capacitance of this kind of SWNT fibrils also indicates that they have a large specific surface area. Furthermore, SWNTs have very fast interfacial electron transfers.[26] Since no polymer or surfactant was used in the fabrication of the CNT fibrils in our experiment, only CNTs are on the surface of the fibrils. We expect that such CNT fibrils will have great potentials for applications as biosensors and bioelectrodes.[5,27−30] Such nanoelectrodes can be used to detect chemical substance at a nano- to picomolar concentration in solutions.[28,31]

The electrical conductivity of the prepared long SWNT fibrils was measured using both the two-probe and the four-probe methods. A long SWNT fibril was placed on a glass slide and fixed with silver paste at both ends and the testing point in the experimental setup. By comparing the current−voltage ($I-V$) curves for the two configurations, we found that no significant difference existed between the results from the two-probe measurement and the four-probe measurement, indicating that the contact resistance between the fibril and the silver paste in our experiment is insignificant for such long fibrils. In addition, the contact area between the fibril and the silver paste is so large that the contact resistance had actually been reduced to a very low value. The resistance of the tested fibril, shown in Figure 4a, was calculated to be 161.0 ± 0.7 kΩ, and the conductivity was estimated to be 80 S cm^{-1}. From the SEM images, we also observed that the thicker fibril had many pores on the surface. All of the $I-V$ curves at low voltage (<10 V) looked quite linear, and the squared correlation coefficient (R^2) was close to 1.

However, it is different when the $I-V$ relationship is tested at higher voltages. After the voltage is increased to more than 10 V, the resistance of the CNT fibrils will reduce nonlinearly as the current increases. A typical $I-V$ curve by the two-probe method is shown in Figure 4b. The resistance dropped from 130 kΩ to below 90 kΩ (by about 30%). The high current would eventually burn the CNT fibril when the maximum current density is reached. We also found that the maximum current was related to the diameter of the CNT fibrils, and the maximum current density could be as high as 10^5 A cm^{-2}. The SEM images revealed the detailed structure of the CNT fibril at the broken point (Figure 5). The conductivity experiments were repeated for more than five samples with different diameters. The conductivity ranged from 80 to 200 S cm^{-1}. Every sample was examined using SEM after burn off. It is observed that one end is always very sharp and the other is a little blunt in contrast.

Though individual SWNTs have excellent electrical properties and the current-carrying capacity of metallic SWNTs can be 1000 times larger than that of copper,[14,32] the structural defects, impurities, and semiconducting CNTs present in the assembled SWNT fibrils are expected to reduce significantly the electrical conductivity and current-carrying capacity. Nonetheless, the maximum current density carried by the SWNT fibrils prepared in our experiment is still comparable to that of a copper wire. Besides the defects and pores, the

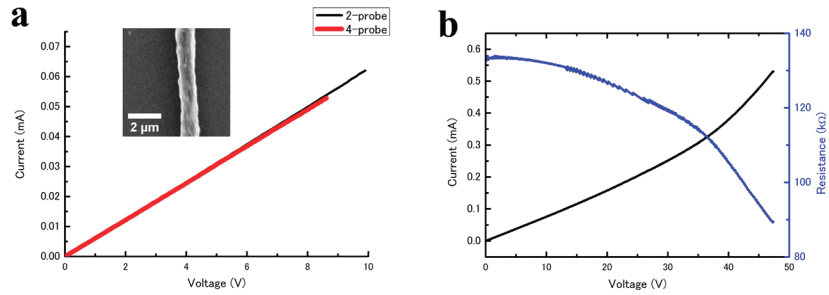

Figure 4. Typical $I-V$ curves of the SWNT fibrils. (a) Comparison of $I-V$ curves between four-probe and two-probe measurements on the same part of a fibril. The inset is an SEM image of the fibril after the $I-V$ measurements. (b) $I-V$ and $R-V$ curves of a fibril using the two-probe method, and the fibril broke after the voltage reached 47.4 V.

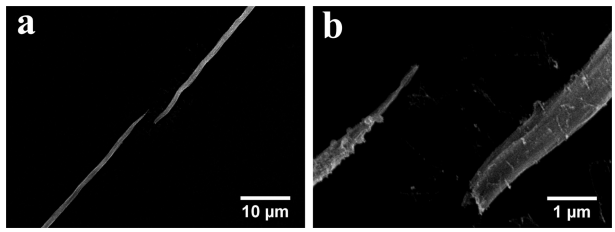

Figure 5. SEM images of the broken point. (a) Low-magnification image of the broken fibril and (b) magnified image showing that the broken point formed a sharp end and a blunt end, respectively.

other reasons for the reduced electrical conductivity of the produced fibrils are related to the SWNT quality, length, and alignment. Because the individual SWNTs have very high current-carrying capacity, the SWNT fibrils are of great potential for improvement if SWNTs of higher quality are used as the starting material.[3] However, the contact areas between the SWNTs cannot bear large current, resulting in a lower maximum current density compared to the short and thin CNT bundles. Similarly, the intertubular contacts also contribute significantly to the increased electrical resistance. We suggest that the electrical resistivity would be further lowered when longer and better aligned SWNT bundles are used in preparing the SWNT fibrils.

The reduction of electrical resistance with increasing voltage is attributed to the electrostriction effects. Higher electrical current will lead to more and closer contact between the SWNT bundles due to the presence of an enhanced electrical field. On the other hand, when the electrical field is higher than the threshold value, the fibril would be pulled apart at a weaker point. It is also interesting to note that the breaking process is very fast.

CONCLUSIONS

We have prepared long SWNT fibrils of submicrometer diameter without any additive agents by dielectrophoresis. These kinds of ultrathin CNT long fibrils have improved mechanical strength and electrical conductivity as well as high electrochemical sensitivity required for many biological applications as conductive thin wires and biological probe electrodes.

METHODS

The experimental setup for preparing the SWNT fibrils is similar to the system described before.[19,20] A three-dimensional motorized stage controlled by a computer was used instead of the manual manipulator. A tungsten tip prepared by chemical etching was used as the working electrode and a small metal ring as the counter electrode, and the tungsten tip was mounted on the motorized stage. The movement is controlled using a Lab View program. The metal ring is mounted on another stage. A high-resolution optical digital microscope is used to monitor the drawing process.

SWNTs (purchased commercially from CheapTubes, Inc.) were first purified, cut, and then dispersed in deionized water.[33] The drawing speed of the tungsten tip is set and controlled by the computer. A functional generator is used to supply the high-frequency (2 MHz) AC voltage of 10 V (peak-to-peak).

SEM images were acquired using a JSM-6500 field-emission scanning electron microscope (FE-SEM). Samples for FE-SEM observations were dried in air overnight.

CV was performed using a potentiostat/galvanostat (CH151, Hokuto-Denko). The scanning triangle waveform was produced by a functional generator. The specific capacitance is calculated from the CV curves by $C_g = I/(m\nu)$, where C_g is the specific electric double layer capacitance (F g^{-1}), I is the electrical current (A), m is the mass of the SWNT fibril, estimated by its density (1 g cm^{-3}) and the measured physical dimensions, and ν is the potentiostat scan rate (V s^{-1}). The positive current at 0.4 V was used in the calculations.[25]

Electrical conductivity measurements were carried out at room temperature. A Keithley 6517B electrometer was used to conduct the staircase scanning program to obtain the $I-V$ curves (two-probe method). For the four-probe measurement, an additional Keithley 2000 electrometer was used to obtain the voltage value on the tested fibril.

Acknowledgment. We thank financial support from JSPS Grants-in-Aid for Scientific Research No. 19710101, Research for Promoting Technological Seeds (2008) of Japan Science and Technology Corporation (JST), and the Nanotechnology Network Project of the Ministry of Education, Culture, Sports, Science and Technology (MEXT), Japan.

REFERENCES AND NOTES

1. Iijima, S.; Ichihashi, T. Single-Shell Carbon Nanotubes of 1-nm Diameter. *Nature* **1993**, *364*, 737.
2. Baughman, R. H.; Zakhidov, A. A.; de Heer, W. A. Carbon Nanotubes—The Route toward Applications. *Science* **2002**, *297*, 787–792.
3. Anantram, M. P.; Leonard, F. Physics of Carbon Nanotube Electronic Devices. *Rep. Prog. Phys.* **2006**, *69*, 507–561.
4. Koziol, K.; Vilatela, J.; Moisala, A.; Motta, M.; Cunniff, P.; Sennett, M.; Windle, A. High-Performance Carbon Nanotube Fiber. *Science* **2007**, *318*, 1892–1895.
5. Pumera, M. The Electrochemistry of Carbon Nanotubes: Fundamentals and Applications. *Chem.—Eur. J.* **2009**, *15*, 4970–4978.
6. Yu, M. F.; Files, B. S.; Arepalli, S.; Ruoff, R. S. Tensile Loading of Ropes of Single Wall Carbon Nanotubes and Their Mechanical Properties. *Phys. Rev. Lett.* **2000**, *84*, 5552–5555.
7. Niyogi, S.; Hamon, M. A.; Hu, H.; Zhao, B.; Bhowmik, P.; Sen, R.; Itkis, M. E.; Haddon, R. C. Chemistry of Single-Walled Carbon Nanotubes. *Acc. Chem. Res.* **2002**, *35*, 1105–1113.
8. Baughman, R. H.; Cui, C. X.; Zakhidov, A. A.; Iqbal, Z.; Barisci, J. N.; Spinks, G. M.; Wallace, G. G.; Mazzoldi, A.; De Rossi, D.; Rinzler, A. G.; *et al.* Carbon Nanotube Actuators. *Science* **1999**, *284*, 1340–1344.
9. Li, N. Q.; Wang, J. X.; Li, M. X. Electrochemistry at Carbon Nanotube Electrodes. *Rev. Anal. Chem.* **2003**, *22*, 19–33.
10. Smart, S. K.; Cassady, A. I.; Lu, G. Q.; Martin, D. J. the Biocompatibility of Carbon Nanotubes. *Carbon* **2006**, *44*, 1034–1047.
11. Harrison, B. S.; Atala, A. Carbon Nanotube Applications for Tissue Engineering. *Biomaterials* **2007**, *28*, 344–353.
12. Poulin, P.; Vigolo, B.; Launois, P. Films and Fibers of Oriented Single Wall Nanotubes. *Carbon* **2002**, *40*, 1741–1749.
13. Zhang, M.; Atkinson, K. R.; Baughman, R. H. Multifunctional Carbon Nanotube Yarns by Downsizing an Ancient Technology. *Science* **2004**, *306*, 1358–1361.
14. Behabtu, N.; Green, M. J.; Pasquali, M. Carbon Nanotube-Based Neat Fibers. *Nano Today* **2008**, *3*, 24–34.
15. Davis, V. A.; Ericson, L. M.; Parra-Vasquez, A. N. G.; Fan, H.; Wang, Y. H.; Prieto, V.; Longoria, J. A.; Ramesh, S.; Saini,

R. K.; Kittrell, C.; *et al.* Phase Behavior and Rheology of SWNTs in Superacids. *Macromolecules* **2004**, *37*, 154–160.
16. Spinks, G. M.; Mottaghitalab, V.; Bahrami-Saniani, M.; Whitten, P. G.; Wallace, G. G. Carbon-Nanotube-Reinforced Polyaniline Fibers for High-Strength Artificial Muscles. *Adv. Mater.* **2006**, *18*, 637–640.
17. Lynam, C.; Moulton, S. E.; Wallace, G. G. Carbon-Nanotube Biofibers. *Adv. Mater.* **2007**, *19*, 1244–1248.
18. Razal, J. M.; Gilmore, K. J.; Wallace, G. G. Carbon Nanotube Biofiber Formation in a Polymer-Free Coagulation Bath. *Adv. Funct. Mater.* **2008**, *18*, 61–66.
19. Tang, J.; Gao, B.; Geng, H. Z.; Velev, O. D.; Qin, L. C.; Zhou, O. Assembly of 1D Nanostructures into Sub-Micrometer Diameter Fibrils with Controlled and Variable Length by Dielectrophoresis. *Adv. Mater.* **2003**, *15*, 1352–1355.
20. Zhang, J.; Tang, J.; Yang, G.; Qiu, Q.; Qin, L. C.; Zhou, O. Efficient Fabrication of Carbon Nanotube Point Electron Sources by Dielectrophoresis. *Adv. Mater.* **2004**, *16*, 1219–1222.
21. Tang, J.; Yang, G.; Zhang, Q.; Parhat, A.; Maynor, B.; Liu, J.; Qin, L. C.; Zhou, O. Rapid and Reproducible Fabrication of Carbon Nanotube AFM Probes by Dielectrophoresis. *Nano Lett.* **2005**, *5*, 11–14.
22. Kim, J. E.; Han, C. S. Use of Dielectrophoresis in the Fabrication of an Atomic Force Microscope Tip with a Carbon Nanotube: A Numerical Analysis. *Nanotechnology* **2005**, *16*, 2245–2250.
23. Wei, H. Y.; Craig, A.; Huey, B. D.; Papadimitrakopoulos, F.; Marcus, H. L. Electric Field and Tip Geometry Effects on Dielectrophoretic Growth of Carbon Nanotube Nanofibrils on Scanning Probes. *Nanotechnology* **2008**, *19*, 455303.
24. Krupke, R.; Hennrich, F.; von Lohneysen, H.; Kappes, M. M. Separation of Metallic from Semiconducting Single-Walled Carbon Nanotubes. *Science* **2003**, *301*, 344–347.
25. Suppiger, D.; Busato, S.; Ermanni, P. Characterization of Single-Walled Carbon Nanotube Mats and Their Performance as Electromechanical Actuators. *Carbon* **2008**, *46*, 1085–1090.
26. Heller, I.; Kong, J.; Heering, H. A.; Williams, K. A.; Lemay, S. G.; Dekker, C. Individual Single-Walled Carbon Nanotubes as Nanoelectrodes for Electrochemistry. *Nano Lett.* **2005**, *5*, 137–142.
27. Campbell, J. K.; Sun, L.; Crooks, R. M. Electrochemistry Using Single Carbon Nanotubes. *J. Am. Chem. Soc.* **1999**, *121*, 3779–3780.
28. Huang, W. H.; Pang, D. W.; Tong, H.; Wang, Z. L.; Cheng, J. K. A Method for the Fabrication of Low-Noise Carbon Fiber Nanoelectrodes. *Anal. Chem.* **2001**, *73*, 1048–1052.
29. Kovalyuk, Z. D.; Motsnyi, F. V.; Zinets, O. S.; Yurcenyuk, S. P.; Tamburri, E.; Orlanducci, S.; Guglielmotti, V.; Toschi, F.; Terranova, M. L.; Rossi, M. An Innovative and Viable Route for the Realization of Ultra-Thin Supercapacitors Electrodes Assembled with Carbon Nanotubes. *J. Nanosci. Nanotechnol.* **2009**, *9*, 2124–2127.
30. Grundler, P.; Frank, O.; Kavan, L.; Dunsch, L. Carbon Nanotube Electrodes for Hot-Wire Electrochemistry. *Chemphyschem* **2009**, *10*, 559–563.
31. Mahmoud, K. A.; Hrapovic, S.; Luong, J. H. T. Picomolar Detection of Protease Using Peptide/Single Walled Carbon Nanotube/Gold Nanoparticle-Modified Electrode. *ACS Nano* **2008**, *2*, 1051–1057.
32. Kasumov, A. Y.; Deblock, R.; Kociak, M.; Reulet, B.; Bouchiat, H.; Khodos, I. I.; Gorbatov, Y. B.; Volkov, V. T.; Journet, C.; Burghard, M. Supercurrents through Single-Walled Carbon Nanotubes. *Science* **1999**, *284*, 1508–1511.
33. Zhou, O.; Shimoda, H.; Gao, B.; Oh, S. J.; Fleming, L.; Yue, G. Z. Materials Science of Carbon Nanotubes: Fabrication, Integration, and Properties of Macroscopic Structures of Carbon Nanotubes. *Acc. Chem. Res.* **2002**, *35*, 1045–1053.